

Analysis of O-Glycans by Oxidative Release Combined with 3-Nitrophenylhydrazine Derivatization

Zhenghu Min, Xingdan Wang, Xiaoqiu Yang, Qiwei Zhang,* and Qi Zheng



Cite This: *ACS Omega* 2025, 10, 14403–14412



Read Online

ACCESS |



Metrics & More

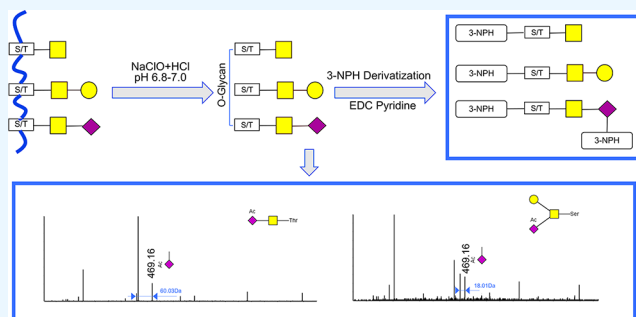


Article Recommendations



Supporting Information

ABSTRACT: Glycosylation profiling is an effective methodology for achieving a comprehensive understanding of glycoproteins and their alterations in a multitude of pathological conditions. However, in comparison to *N*-glycosylation, *O*-glycosylation presents significant challenges in terms of both qualitative and quantitative mass spectrometric analyses. A recently developed oxidative release protocol enables the selective formation of *O*-glycans containing a carboxyl group derived from the amino acid residue. In this study, 3-nitrophenylhydrazine was used to derivatize the common carboxyl group in a mild hydrophilic solution. Derivatization resulted in the generation of a series of report ions for serine, threonine, sialic acid, and *O*-acetylated sialic acid residues, thereby facilitating the identification of *O*-glycans and their attached amino acid residues, as well as the determination of the number of *O*-acetyl groups. A total of 65 *O*-glycans can be identified from bovine mucin. Furthermore, the analytical strategy revealed that *O*-acetylated *N*-acetylneuraminic acid (Neu5Ac)-containing *O*-glycans from horse serum exhibited distinctive fragmentation patterns in comparison to those from bovine mucin. Additionally, the presence of deaminoneuraminic acid (KDN)-containing *O*-glycans was successfully confirmed in fish intestinal tissue. These findings suggest that this method provides an economical and potentially valuable tool for large-scale *O*-glycosylation studies in complex biological samples.



1. INTRODUCTION

Proteins are the primary executors of life activities, and a significant proportion of proteins require activation or regulation by post-translational modifications (PTMs). Glycosylation represents one of the most prevalent and diverse PTMs, with evidence suggesting that more than 50% of human proteins undergo this modification.¹ These glycoproteins play important roles in key biological processes, including protein interactions, molecular recognition, immune response, and signal transduction.^{2–4} The most common types of glycosylation are *N*-glycosylation and *O*-glycosylation. *N*-glycosylation is a process whereby *N*-glycans are covalently attached to the Asn residue of a specific peptide sequence (Asn-X-Ser/Thr, where X is any amino acid other than Pro) via a series of glycosyltransferases.⁵ While *O*-glycans are typically attached to the Ser/Thr residue without any discernible sequence pattern. Additionally, in contrast to *N*-glycosylation, *O*-glycosylation allows for the direct linkage of a variety of monosaccharides to proteins, including *N*-acetylgalactosamine (GalNAc), *N*-acetylglucosamine (GlcNAc), mannose (Man), glucose (Glc), and fucose (Fuc).^{6,7}

At the molecular level, *O*-glycosylation plays a crucial role in ensuring the correct folding of proteins and enhancing protein stability, which is vital for preserving the integrity of secretory proteins or membrane proteins within the extracellular matrix or cellular membranes.⁸ At the cellular level, *O*-glycosylation plays a role in the regulation of cellular adhesion.⁹ The interaction of

glycoproteins with cell surface molecules and extracellular components is facilitated by *O*-glycans, which are essential for the processes of tissue and organ formation. And the *O*-glycans in cell surface glycoproteins can influence the binding affinity and delivery efficiency of growth factor receptors, as well as regulating cell proliferation, differentiation, and survival.^{8,10} Additionally, it has been demonstrated that *O*-glycosylation exerts a significant influence on the interactions between immune cells and antigens, as well as the initiation of the immune response.¹¹ At the disease level, aberrant *O*-glycosylation processes are frequently observed, particularly in cancer, neurodegenerative diseases, and autoimmune diseases. Such aberrant patterns may serve as biomarkers for the diagnosis and prognosis of diseases.^{12,13}

Accordingly, the localization and identification of *O*-glycans represent a fundamental aspect of elucidating their biological properties and obtaining biomarkers. At present, mass spectrometry (MS)-based analytical techniques have become

Received: January 21, 2025

Revised: March 12, 2025

Accepted: March 27, 2025

Published: April 3, 2025



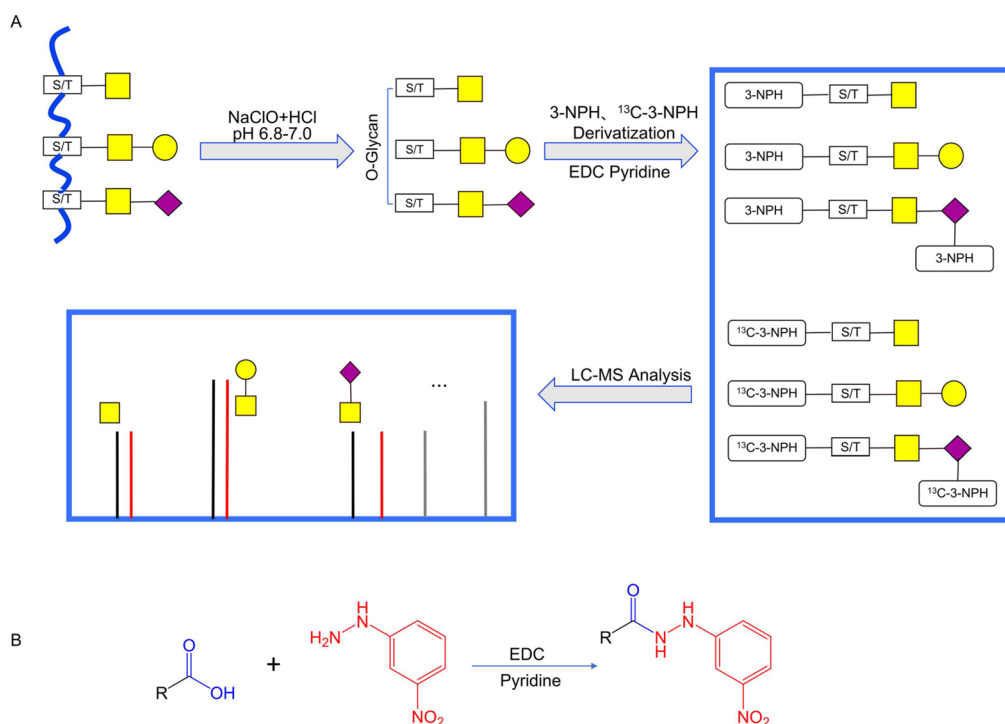


Figure 1. Diagram showing the steps for analyzing O-glycans. (A) Workflow for the analysis using oxidative release and 3-NPH derivatization, followed by LC–MS; (B) the derivatization scheme for carboxyl group.

the primary tool for the study of glycosylation.¹⁴ However, in contrast to the well-established methods for *N*-glycosylation, O-glycomics remains a relatively underdeveloped field of research.^{15,16} This is primarily due to the absence of a universal enzyme capable of cleaving diverse glycans from serine or threonine residues, the use of alkaline β -elimination, which is a common approach for the release of O-glycans, being prone to result in peeling reactions, and the constraints of typical labeling methods (e.g., reducing amination labeling).^{17,18} To some extent, these issues are gradually being addressed and resolved. A previous study demonstrated that hypochlorite-based oxidation represents an economical and scalable method for the release of *N*-glycans, O-glycans, and glycolipids from proteins.¹⁹ Further research indicated that O-glycans can be released in a selective manner by neutralized hypochlorite (pH = 6.8–7.0). The oxidation release enables the distinctive information on the parent amino acid (Ser/Thr) to be preserved, resulting in the formation of lactate/glycolic acid-linked O-glycans. And this process effectively secures the glycans in a closed-loop conformation, thereby preventing the generation of peeling reactions. In short, the methodology based on neutralized oxidation release not only circumvents the limitations of alkaline β -elimination but also yields oligosaccharides containing a carboxyl group derived from the Ser/Thr residue. The presence of the common carboxyl group provides an additional derivatization site, thus enabling the application of nonreductive amination labeling techniques to O-glycans.²⁰

The majority of established derivatization approaches for oligosaccharides are constrained to nonaqueous solvents or harsh reaction conditions. However, recent studies have demonstrated that 3-nitrophenylhydrazine (3-NPH) dissolved in a mixture of water and methanol can rapidly derivatize carboxyl and carbonyl metabolites via a mild reaction.^{21,22} The method exhibits satisfactory sensitivity, stability, and reproducibility for large-scale sample analysis. In light of these findings,

this study employed oxidative release and 3-NPH derivatization combined with LC–MS for the analysis of O-glycans from biological samples. Following optimization, the neutralized hypochlorite-based method was demonstrated to be an effective means of releasing O-glycans from serum and tissue samples. And following the derivatization of the carboxyl groups present in both the Ser/Thr residue and sialic acid residues, a change in the fragmentation pattern of O-glycans was observed during tandem MS (MS/MS) analysis. As a result, reporter ions were generated for oligosaccharides containing a Ser/Thr residue, as well as those containing sialic acids or O-acetylated sialic acid residues. Moreover, differences were identified between the MS/MS spectra of O-glycans bearing 4-O-acetylated sialic acid and those containing alternative O-acetylation. These findings suggest that the oxidative release protocol in conjunction with 3-NPH derivatization may represent an effective approach for the analysis of O-glycosylation in complex biological samples.

2. EXPERIMENT

2.1. Chemicals and Materials. Bovine submaxillary mucin, radioimmunoprecipitation assay (RIPA) buffer II, and horse serum were from Sangon Biotech (Shanghai, China). Formic acid (FA, LC–MS grade) and dimethyl sulfoxide (DMSO) were purchased from Sigma-Aldrich (St. Louis, USA). Acetonitrile (ACN, LC–MS grade), methanol (MeOH), ethanol, trichloromethane (CHCl₃), sodium dodecyl sulfate (SDS), sodium hypochlorite (NaClO) solution ($\geq 8\%$ active chlorine), hydrochloric acid (HCl), trifluoroacetic acid (TFA), 3-NPH, 1-ethyl-3-(3-(dimethylamino)propyl)carbodiimide (EDC), and pyridine were purchased from Aladdin (Shanghai, China). The ¹³C-substituted 3-NPH (¹³C-3-NPH) was ordered from MedBio (Shanghai, China). The porous graphitized carbon (PGC) and C18 cartridges were from Biocomma (Shenzhen,

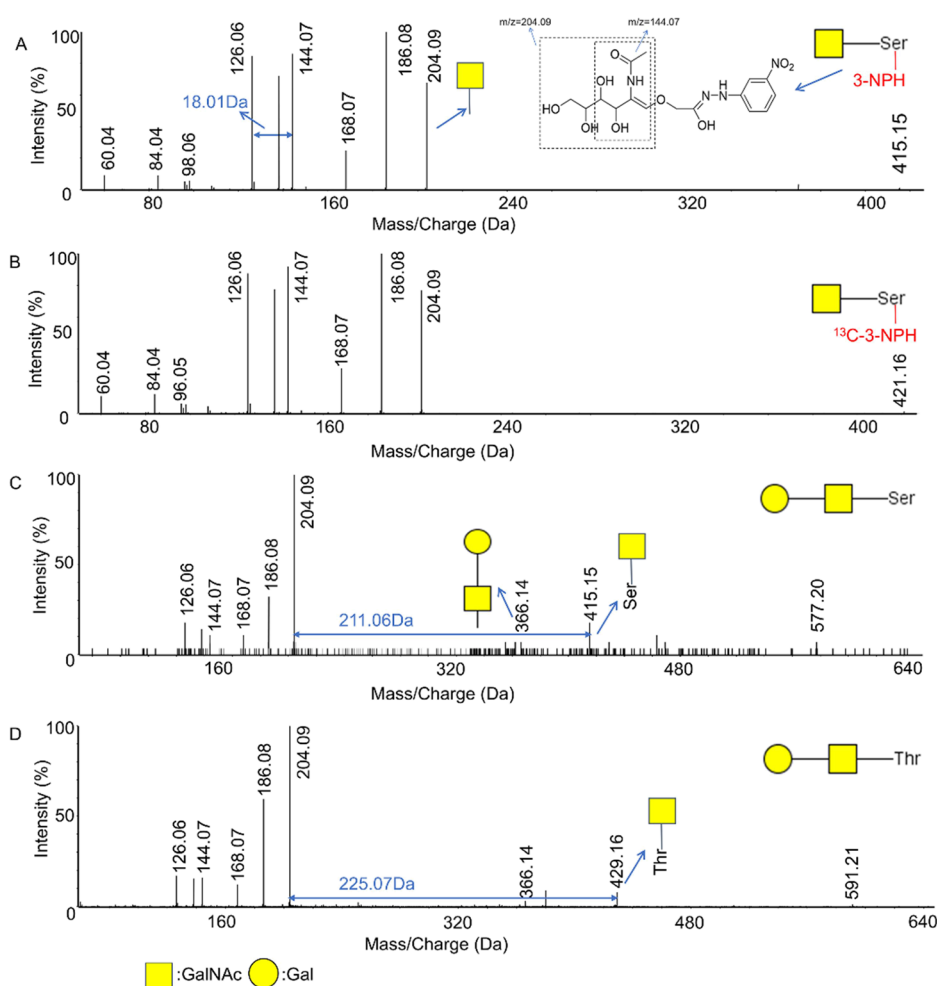


Figure 2. Fragmentation patterns of several O-glycans released from bovine mucin. (A) MS/MS spectrum for 3-NPH-labeled GalNAc-Ser; (B) MS/MS spectrum for ^{13}C -3-NPH-labeled GalNAc-Ser; MS/MS spectra for 3-NPH-labeled Gal-GalNAc-Ser (C) and Gal-GalNAc-Thr (D), respectively.

China). The goldfish (*Carassius auratus*) fries (approximately 7 cm in length) were obtained from a local market.

2.2. Sample Preparation. A pooled sample comprising intestinal tissues from three goldfish was prepared. Each tissue sample, with a wet weight of approximately 40 mg, was homogenized in 400 μL of RIPA buffer II. Subsequently, the lysate was subjected to vacuum drying and extracted in sequence with 400 μL of $\text{CHCl}_3/\text{MeOH}$ (2:1, v/v) and 400 μL of $\text{CHCl}_3/\text{MeOH}$ (1:2, v/v).²³ The resulting precipitation was dissolved in 400 μL of 0.3% SDS (w/w), and the protein concentration was then determined. A portion of the solution, equivalent to 2 mg of tissue protein, was diluted with 0.3% SDS to a volume of 500 μL . A solution of 750 μL of NaClO, adjusted to a pH of 6.8–7.0 with 1 M HCl, was mixed with the sample, followed by an incubation at 4 $^\circ\text{C}$ for 2 h. The reaction was terminated by the addition of 3 μL of FA. The sample solution was loaded into a PGC cartridge and washed with 2.0 mL of 0.1% TFA (v/v). The released O-glycans were eluted with 1.0 mL of 40% ACN (containing 0.1% TFA, v/v). A 20 μL aliquot of horse serum was directly diluted with 500 μL of 0.3% SDS, and the subsequent treatment was identical to that employed for fish tissue samples.

The dried sample was redissolved in 100 μL of 70% MeOH (v/v), then mixed with 50 μL of 0.2 M 3-NPH in 70% MeOH (containing 6% pyridine, v/v) and 50 μL of 0.12 M EDC in 70% MeOH (v/v).²² The mixture was then incubated at room temperature for 75 min, after which vacuum drying was

performed. The sample was redissolved in 1.0 mL of 5% DMSO (v/v) and subsequently loaded into a C18 cartridge. The cartridge was rinsed with 2.0 mL of water, and the derivatized glycans were extracted with 1.0 mL of 50% ethanol (v/v), followed by vacuum drying.

2.3. MicroLC–MS Analysis. Sample detection was conducted using an M5 microLC coupled to a TripleTOF 5600+ mass spectrometer (SCIEX, USA) with electrospray ionization. The microLC system was equipped with a Phenomenex Kinetex C18 column (2.6 μm , 0.3 mm \times 150 mm, USA), maintained at 45 $^\circ\text{C}$. The flow rate was set to 6 $\mu\text{L}/\text{min}$, with 0.1% FA in water (v/v) as mobile phase A and ACN as mobile phase B. The gradient elution was programmed as follows: 5% B (0–2 min), 5–45% B (2–30 min), 45–95% B (30–33 min), 95% B (33–39 min), and 95–5% B (39–41 min). The mass spectrometer was operated in positive ion mode with the following settings: an ion source gas 1 (N_2) pressure of 17 psi, an ion source gas 2 (N_2) temperature of 300 $^\circ\text{C}$ and pressure of 18 psi, and a spray voltage of 5500 V. The MS/MS data were acquired using a collision energy of 30 ± 5 V. The data were analyzed with PeakView software (version 2.2), and the peak area for each O-glycan was extracted based on its theoretical m/z that was calculated with GlycoWorkbench software (version 2.1), with an error of ± 0.02 Da (Figure S1).

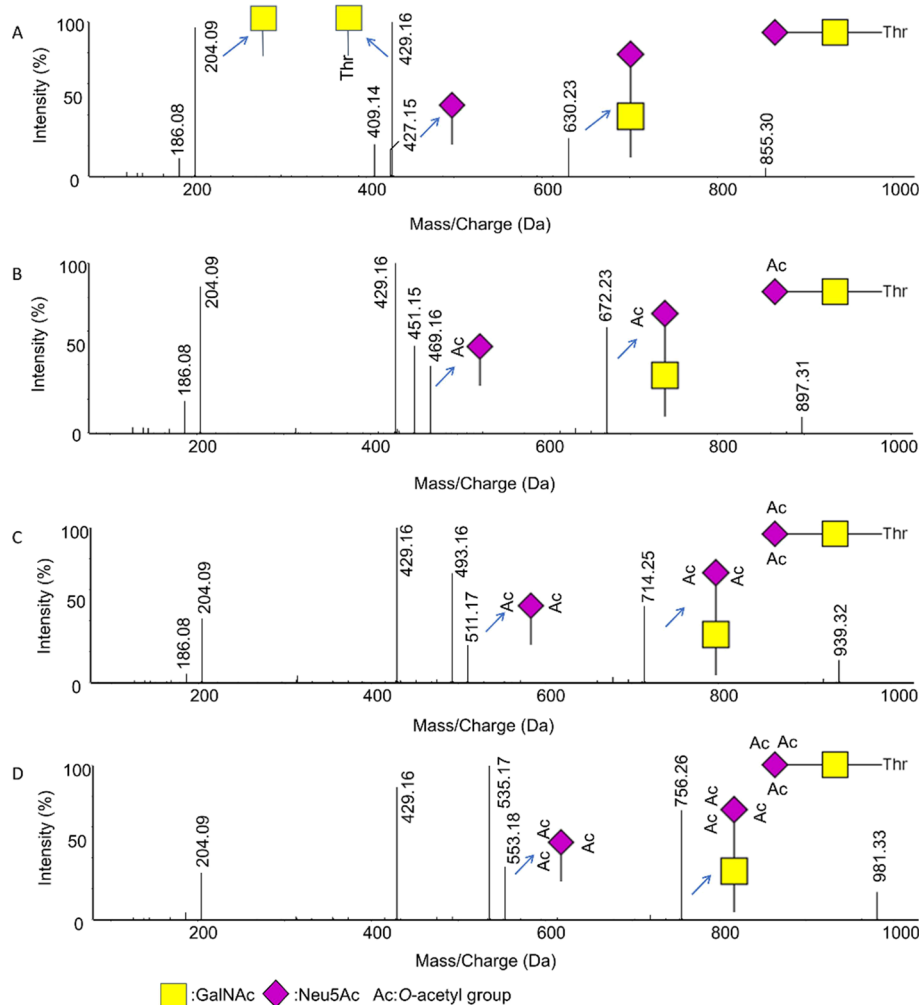


Figure 3. Fragmentation patterns of sialylated *O*-glycans released from bovine mucin. MS/MS spectra for Neu5Ac-GalNAc-Thr (A), Neu5Ac₂-GalNAc-Thr (B), Neu5Ac₃-GalNAc-Thr (C), and Neu5Ac₄-GalNAc-Thr (D), respectively.

3. RESULTS

3.1. Workflow for Analyzing *O*-Glycans. The methodology utilized for the analysis of *O*-glycans is illustrated in Figure 1. The neutral sodium hypochlorite is employed to cleave proteins, resulting in the selective formation of *O*-glycans containing a Ser or Thr residue. Derivatization of both carboxyl groups from the amino acid and sialic acid residues can be achieved through the use of 3-NPH or ¹³C-3-NPH. The application of isotope labeling results in a molecular weight difference of 6.02 Da for each label. Moreover, the product ion bearing a 3-NPH label can also exhibit a difference of 6.02 Da in MS/MS analysis, which facilitates the identification of *O*-glycans.

3.2. *O*-Glycans from Mucin. Mucin is a highly glycosylated protein that is linked with numerous *O*-glycan chains. Accordingly, it was selected for experimental analysis with the objective of elucidating the features of the derivatized *O*-glycans. For example, the MS/MS spectra for a simple *O*-glycan with an *m/z* of 415.15 Da for 3-NPH labeling and 421.17 Da for ¹³C-3-NPH labeling are presented in Figure 2a,b, respectively. No notable distinction is observed between the two MS/MS spectra, indicating that the primary product ions are not influenced by the 3-NPH label. The observed *m/z* of 204.09 Da indicates the presence of acetylhexosamine residue in the

precursor ion. Therefore, this glycan was identified as GalNAc-Ser. Due to the abundance of hydroxyl groups present in *O*-glycans, a neutral loss may occur during the dissociation. It can thus be inferred that the fragments at *m/z* 186.08 and 168.07 Da correspond to the products resulting from the neutral loss of the GalNAc residue. Additionally, it is well documented that following the collision of molecules with inert gases, the bonds with the lowest energies are preferentially cleaved. These include bonds between carbon and carbon, carbon and nitrogen, and carbon and oxygen. In light of these factors, the product ions at *m/z* 144.07 and 126.06 Da are attributed to the secondary cleavage within the GalNAc residue. Moreover, these ions are also observed in the MS/MS spectra for GalNAc-Thr (Figure S2). It can thus be concluded that the fragments at *m/z* 204.09 and 144.06 Da can be employed as reporter ions for acetylhexosamine-containing glycans.

Given that GalNAc-Ser/Thr represents a common structural motif among mucin *O*-glycans, the product ions at *m/z* 415.15 and 429.16 Da can be employed as reporter ions for the differentiation between GalNAc-Ser-type and GalNAc-Thr-type glycans. Furthermore, they are capable of yielding distinct fragments with a reduced mass weight of 211.06 and 225.07 Da, respectively. These values correspond to the anticipated mass weight of 3-NPH-labeled Ser and Thr residues. The aforementioned ions facilitate the rapid identification of the

amino acids attached to O-glycans, thus providing a convenient method for the evaluation of differences in Ser- and Thr-linked O-glycans.

Sialylation endows the O-glycan with distinctive structural properties, enabling it to serve as the initial point of contact with external molecules.²⁴ The most common sialic acids engaged in O-glycosylation are *N*-acetylneuraminic acid (Neu5Ac) and *N*-glycolylneuraminic acid (Neu5Gc). They are frequently attached to the end of O-glycans and may undergo additional modifications, such as *O*-acetylation. In this study, it was found that a series of mono-sialylated mucin O-glycans exhibit a comparable fragmentation pattern. Typically, the product ions with a sequential increase of 42.01 Da (427.15, 469.16, 511.17, and 553.18 Da; 630.23, 672.24, 714.25, and 756.26 Da) can be observed in their MS/MS spectra (Figure 3). This indicates that the O-glycans in question contain between zero and three *O*-acetyl groups linked with the Neu5Ac residue. The MS/MS spectra for the O-glycans containing *O*-acetylated Neu5Gc residues display analogous characteristics (Figure S3). Moreover, it is noteworthy that Figures 3 and S2 demonstrate that the derivatized sialic acid residues exhibit minimal loss of *O*-acetyl groups during collision-induced dissociation, with only a neutral loss of 18.01 Da being observed. This feature allows for the visualization of the quantity of *O*-acetyl groups, thereby reducing the probability of misclassification.

As illustrated in Figures 3a and S2a, the product ions at *m/z* 427.15 and 443.15 Da can be utilized as reporter ions for 3-NPH-labeled Neu5Ac and Neu5Gc, respectively. In contrast, the *m/z* of the reporter ions for their *O*-acetylated forms exhibit a sequential increase of 42.01 Da (Figures 3 and S2). These reporter ions allow for the identification of a variety of sialylated O-glycans from bovine mucin (Table S1). The results demonstrate that over half of the O-glycans have undergone sialylation, with the majority of these glycans also exhibiting *O*-acetylation. Of these, a notable proportion were di- and tri-*O*-acetylated, representing 45% of the Neu5Ac-containing O-glycans. This suggests that even highly unstable acetyl esters at the C-7 or C-8 positions of sialic acids can be retained using the proposed analytical strategy. These findings indicate that oxidative release in conjunction with 3-NPH derivatization represents a promising approach for the analysis of *O*-acetylation profiling of oligosaccharides.

A total of 65 O-glycans, comprising 36 Ser-linked and 29 Thr-linked structures, were identified from 200 μ g of mucin with the assistance of reporter ions (Table S1). Twelve Thr-linked O-glycans were selected for relative quantification based on the peak areas of the extracted ion chromatograms (XICs). The relative standard deviation (RSD) for three replicates is typically less than 20% (Figure 4), thereby demonstrating a high degree of reproducibility associated with this sample preparation method. Moreover, no derivatized O-glycans were observed in either positive or negative ion mode, which indicates that the 3-NPH derivatization process is highly effective. These results, in conjunction with the reporter ions, provide a foundation for the implementation of this approach in the analysis of complex biological samples.

3.3. O-Glycans from Horse Serum. It is a common occurrence for *O*-acetylation to be situated at the C-7, C-8, and C-9 positions of sialic acids. As previously stated, the methodology appears to be effective in preserving these *O*-acetyl groups (Figure 3). In order to determine the viability of employing this analytical strategy to investigate 4-*O*-acetylation, a commercial horse serum sample was utilized in the subsequent

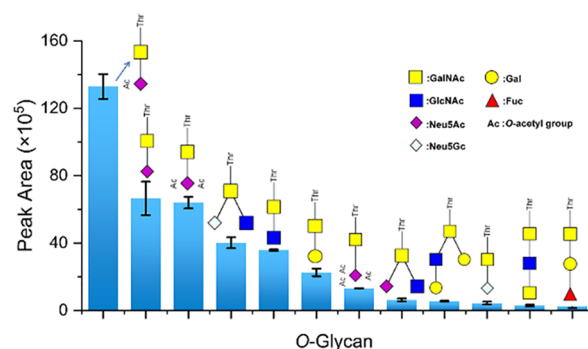


Figure 4. Relative quantitative analysis of select Thr-linked O-glycans from bovine mucin via oxidative release in conjunction with 3-NPH labeling.

study, which has been demonstrated to contain a high abundance of 4-*O*-acetylated Neu5Ac and Neu5Gc.²⁵ As illustrated in Figure 5a, the presence of a product ion at *m/z* 469.16 Da indicates that the glycan contains an *O*-acetylated Neu5Ac residue, which is thus assigned to Neu5Ac₂-(Gal)-GalNAc-Ser. It is noteworthy that no neutral loss of 18.01 Da, associated with this report ion, is observed in the MS/MS spectrum. This differs from the spectra shown in Figure 3. The findings indicate that the method is effective in differentiating between glycans that bear 4-*O*-acetylated sialic acid and those that contain alternative *O*-acetylation.

A total of 11 O-glycans were identified from 20 μ L of horse serum, and the peak area of XICs exhibits a typical RSD of less than 35% (Table 1), indicating that the method is sufficiently stable and effective for serum samples. However, it is evident that the glycans attached to Ser and Thr exhibit notable distinctions, and no glycans containing *O*-acetylated Neu5Gc residues were identified. The underlying causes of these observations may be attributed to a multitude of factors, including the site-specificity of O-glycosylation, the efficacy of neutral hypochlorite in releasing the glycans, and the robust matrix effect afforded by the biological samples. The implementation of an optimized oxidative release protocol or enrichment method may prove beneficial in improving the detection results.

3.4. O-Glycans from Fish Tissue. The goldfish is a model organism with the potential to elucidate the molecular basis of vertebrate development and evolution, as well as to investigate human diseases.²⁶ Accordingly, a further study was conducted using goldfish intestinal tissue to determine the applicability of the method for the analysis of tissue samples. It was observed that the direct application of neutral hypochlorite for the release of oligosaccharides from tissue proteins is markedly inefficient, with only a limited number of O-glycans being detected (data not shown). Thereupon, 0.3% SDS was employed to enhance protein solubility. This resulted in the identification of 19 O-glycans from 2 mg of tissue protein, with an RSD typically less than 30% (Table 2). These findings illustrate that the utilization of suitable protein denaturants can significantly improve the efficacy of oxidative release.

A previous study demonstrated that deaminoneuraminic acid (KDN, 2-keto-3-deoxy-D-glycero-D-galacto-nononic acid) is a highly abundant sialic acid in zebrafish intestinal tissues and microbiota may be accountable for this phenomenon.²⁷ It can thus be postulated that KDN-containing O-glycans should also be present in the intestinal tissues of goldfish. As illustrated in Figure 5b, the product ion at *m/z* 386.12 Da is an indicate of a 3-

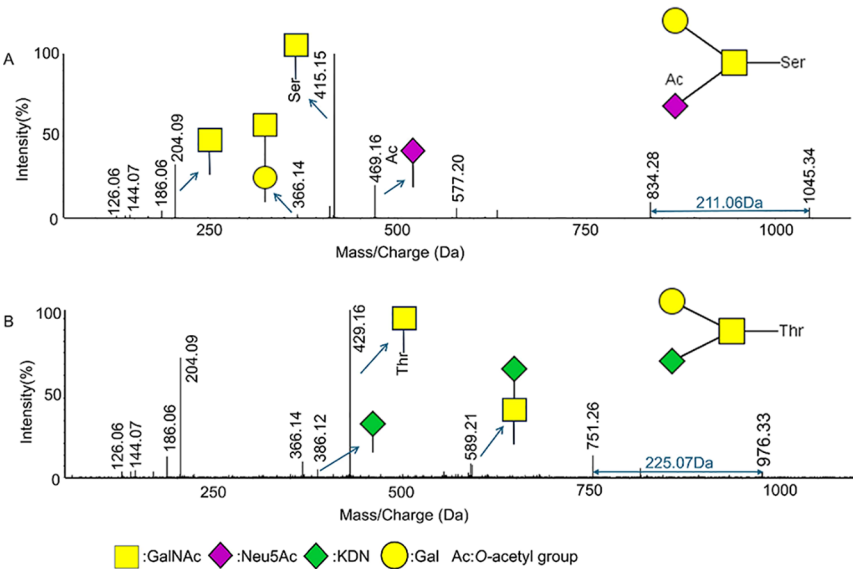




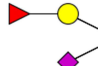
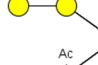







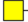


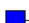



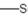















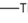
























Figure 5. Fragmentation patterns of sialylated O-glycans in complex biological samples. (A) MS/MS spectrum for 3-NPH-labeled Neu5Ac₂-(Gal)-GalNAc-Ser released from horse serum; (B) MS/MS spectrum for 3-NPH-labeled KDN-(Gal)-GalNAc-Thr released from goldfish intestinal tissues.

Table 1. O-Glycans in Horse Serum: Identification by LC–MS/MS Following Oxidative Release and 3-NPH Derivatization^a

No.	O-Glycan	Precursor ion (m/z)	Average peak area (×10 ⁴ , n = 3)	RSD (%)
1	 -Ser	415.1459	1.61	23.06
2	 -Ser	577.1987	1.24	43.64
3	 -Ser	1003.3374	1.02	22.09
4	 -Ser	1045.3479	3.19	22.77
5	 -Ser	1149.3953	3.72	45.76
6	 -Ser	1207.4007	1.75	26.45
7	 -Thr	429.1615	3.26	25.94
8	 -Thr	591.2143	1.03	45.44
9	 -Thr	855.3001	0.50	15.16
10	 -Thr	1017.3530	0.90	20.40
11	 -Thr	1059.3635	1.64	35.50

^aThe monosaccharide diagram presented in the table is identical to that depicted in Figure 4.

Table 2. O-Glycans in Goldfish Intestinal Tissues: Identification by LC–MS/MS Following Oxidative Release and 3-NPH Derivatization^a

No.	O-Glycan	Precursor ion (m/z)	Average peak area (×10 ⁴ , n = 3)	RSD (%)
1	 –Ser	415.1459	10.33	10.44
2	 –  –Ser	577.1987	1.43	23.40
3	 –  –Ser	632.2409	1.39	20.87
4	 –  –  –Ser	780.2781	0.18	33.11
5	 –  –Ser	800.2580	0.62	20.80
6	 –  –Ser	841.2845	0.73	18.11
7	 –  –Ser  –  –Ser	1044.3639	0.20	14.35
8	 –Thr	429.1615	37.84	10.51
9	 –  –Thr	591.2143	6.08	6.49
10	 –  –Thr	618.2253	3.75	8.81
11	 –  –  –Thr	794.2937	0.88	7.35
12	 –  –Thr	814.2736	2.06	27.42
13	 –  –Thr	855.3001	3.99	19.79
14	 –  –Thr	871.2950	1.46	37.13
15	^{Ac}  –  –Thr	897.3107	0.23	23.29
16	 –  –Thr  –  –Thr	976.3264	0.64	15.62
17	 –  –Thr  –  –Thr	1017.3530	1.43	11.19
18	 –  –Thr  –  –Thr	1033.3479	0.43	8.16
19	 –  –Thr  –  –Thr	1058.3795	2.50	18.20

^aThe monosaccharide diagram presented in the table is identical to that depicted in Figure 4.

NPH-labeled KDN residue. The fragments at *m/z* 204.09, 386.12, and 429.16 Da provide corroboration for the designation of the O-glycan as KDN-(Gal)-GalNAc-Thr. The combination of Figures 3, S2, and 5 illustrates that this approach

enables the generation of individual reporter ions for a range of sialic acids, thereby facilitating rapid and precise characterization of sialylated O-glycans. The XICs from a horse serum sample and a goldfish intestinal sample are presented in Figure 6, in

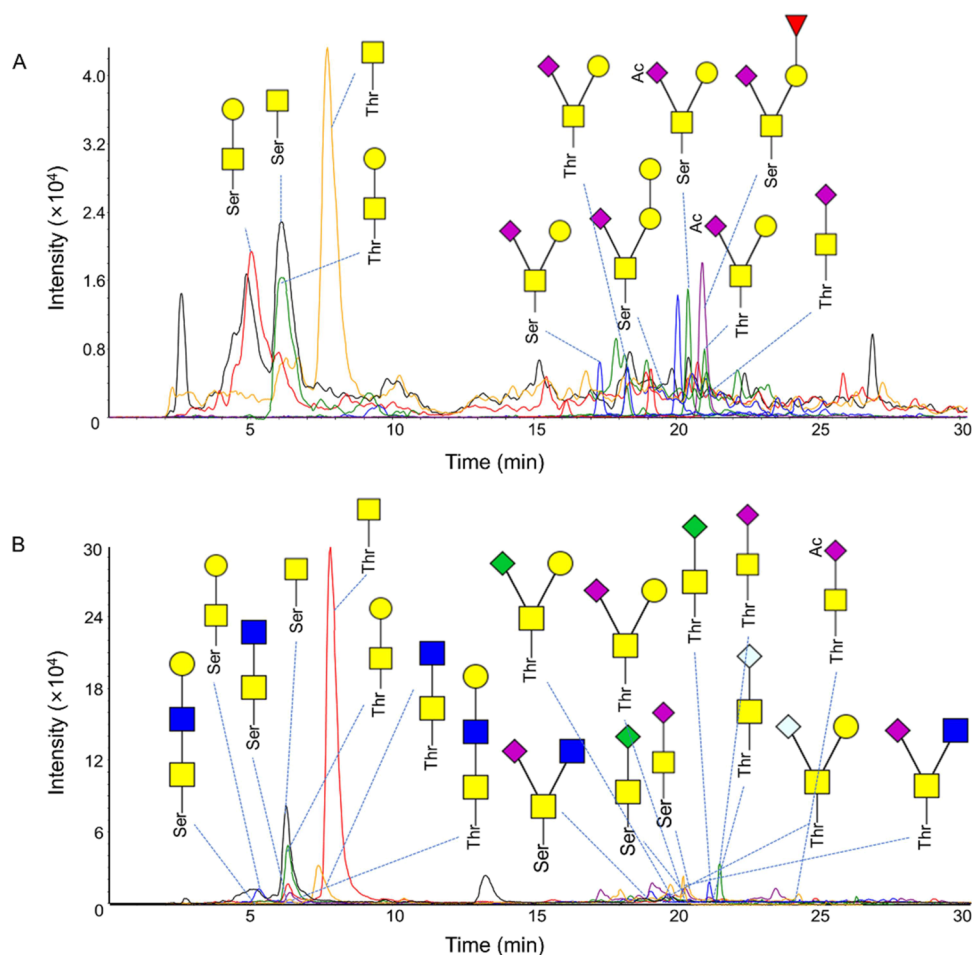


Figure 6. XICs for 3-NPH-labeled O-glycans released from biological samples. (A) The XICs from a horse serum sample; (B) the XICs from a goldfish intestinal sample. The suggested structures presented in the figure are identical to Tables 1 and 2.

accordance with the data presented in Tables 1 and 2, respectively.

4. DISCUSSION

It is imperative to acknowledge the potential occurrence of side reactions during the derivatization process. Figure S4 illustrates two MS/MS spectra for the precursor ions at m/z 734.27 and 750.27 Da, respectively. The fragments at m/z 144.06, 204.09, and 429.16 Da are consistent with the presence of GalNAc-Thr-type O-glycans. However, the product ions at m/z 306.12 and 322.11 Da appear to indicate that they correspond to methylated Neu5Ac and Neu5Gc, respectively, in the absence of a 3-NPH label. In consideration of a preceding study, a hypothesis was formulated proposing that this phenomenon is attributable to the methylation of sialic acid by methanol in the reaction solution.²⁸ The use of acetonitrile or DMSO instead of methanol may mitigate the side reaction. Additionally, an additional charge addition form was observed (Figure S5). The implementation of enhanced desalting strategies is expected to mitigate this issue.

5. CONCLUSIONS

In this study, a protocol for oxidative release in conjunction with 3-NPH derivatization was proposed as a means of profiling protein O-glycosylation. The combination of neutral hypochlorite and a protein denaturant has been demonstrated to facilitate the rapid release of O-glycans from biological samples. The

resulting O-glycans were then derivatized using 3-NPH and subsequently identified via LC–MS/MS analysis. Derivatization resulted in the generation of a series of report ions for serine, threonine, sialic acid (including Neu5Ac, Neu5Gc, and KDN), and O-acetylated sialic acid residues. Notably, O-acetylation was not destroyed during MS/MS analysis, thereby facilitating the determination of the number of O-acetyl groups. Accordingly, the method provides a convenient technique that circumvents the risk of false positives in O-acetylation profiling. The analytical strategy permitted the identification of a total of 65 GalNAc-type O-glycans released from bovine mucin. Moreover, the approach was shown to be effective for examining complex biological samples, and the results demonstrated satisfactory reproducibility. It is noteworthy that O-acetylated Neu5Ac-containing O-glycans from horse serum exhibited distinctive fragmentation patterns in comparison to those from bovine mucin. The observed discrepancy is attributed to the variation in the position of the O-acetyl group. Additionally, the presence of KDN-containing O-glycans was successfully confirmed in intestinal tissue samples from fish.

However, the number of O-glycans identified from tissue samples remains relatively low. The implementation of an optimized oxidative release protocol or enrichment method has the potential to enhance the detection results. And the adoption of alternative solvents may mitigate the side reactions. Nevertheless, this method offers an inexpensive and potentially

valuable tool for large-scale O-glycosylation studies in complex biological samples.

■ ASSOCIATED CONTENT

Supporting Information

The Supporting Information is available free of charge at <https://pubs.acs.org/doi/10.1021/acsomega.5c00652>.

Figure S1: GlycoWorkbench software used to calculate the theoretical m/z for 3-NPH labeled O-glycans; Figure S2: O-glycan GalNAc-Thr exhibits a fragmentation pattern analogous to that observed for GalNAc-Ser; Figure S3: fragmentation pattern exhibited by O-acetylated NeuSGc residues in O-glycans analogous to that observed for O-acetylated NeuSAc residues; Figure S4: MS/MS spectra for the suspected O-glycans containing O-methylated sialic acid residues; Figure S5: XICs for two sialylated O-glycans, released from goldfish intestine and horse serum, respectively; and Table S1: O-glycans in bovine mucin: identification by LC-MS/MS following oxidative release and 3-NPH derivatization. Raw data is stored on the IproX platform and accessed at <https://www.iprox.cn/page/PSV023.html?url=1735108480961qlfv> (PDF)

■ AUTHOR INFORMATION

Corresponding Author

Qiwei Zhang — School of Environment and Health and School of Optoelectronic Materials & Technology, Jiangnan University, Wuhan 430056 Hubei, People's Republic of China; Email: keewezhang@jhun.edu.cn

Authors

Zhenghu Min — School of Environment and Health, Jiangnan University, Wuhan 430056 Hubei, People's Republic of China; orcid.org/0009-0006-9840-8048

Xingdan Wang — School of Optoelectronic Materials & Technology, Jiangnan University, Wuhan 430056 Hubei, People's Republic of China

Xiaoqiu Yang — School of Optoelectronic Materials & Technology, Jiangnan University, Wuhan 430056 Hubei, People's Republic of China

Qi Zheng — School of Optoelectronic Materials & Technology, Jiangnan University, Wuhan 430056 Hubei, People's Republic of China

Complete contact information is available at:

<https://pubs.acs.org/doi/10.1021/acsomega.5c00652>

Notes

The authors declare no competing financial interest.

■ ACKNOWLEDGMENTS

The authors gratefully acknowledge the financial support from the National Natural Science Foundation of China (Grant No. 21976069) and the Research Fund of Jiangnan University (Grant No. 2021KJZX002).

■ REFERENCES

(1) Yang, G. L.; Zhang, H.; Yi, W.; Yan, S.; Cao, L. W. Editorial: protein glycosylation—advances in identification, characterization and biological function elucidation using mass spectrometry. *Front. Chem.* **2022**, *10*, No. 847242.

(2) Pinho, S. S.; Alves, I.; Gaifem, J.; Rabinovich, G. A. Immune regulatory networks coordinated by glycans and glycan-binding proteins in autoimmunity and infection. *Cell. Mol. Immunol.* **2023**, *20* (10), 1101–1113.

(3) Olofsson, S.; Bally, M.; Trybala, E.; Bergström, T. Structure and role of O-linked glycans in viral envelope proteins. *Annu. Rev. Virol.* **2023**, *10*, 283–304.

(4) Schjoldager, K. T.; Narimatsu, Y.; Joshi, H. J.; Clausen, H. Global view of human protein glycosylation pathways and functions. *Nat. Rev. Mol. Cell Biol.* **2020**, *21* (12), 729–749.

(5) Moremen, K. W.; Haltiwanger, R. S. Emerging structural insights into glycosyltransferase-mediated synthesis of glycans. *Nat. Chem. Biol.* **2019**, *15* (9), 853–864.

(6) You, X.; Qin, H. Q.; Ye, M. L. Recent advances in methods for the analysis of protein O-glycosylation at proteome level. *J. Sep. Sci.* **2018**, *41* (1), 248–261.

(7) Bennett, E. P.; Mandel, U.; Clausen, H.; Gerken, T. A.; Fritz, T. A.; Tabak, L. A. Control of mucin-type O-glycosylation: a classification of the polypeptide GalNAc-transferase gene family. *Glycobiology* **2012**, *22* (6), 736–756.

(8) He, M. Y.; Zhou, X. X.; Wang, X. Glycosylation: mechanisms, biological functions and clinical implications. *Signal Transduct. Target. Ther.* **2024**, *9* (1), 194.

(9) Guzman-Arangué, A.; Argüeso, P. Structure and biological roles of mucin-type O-glycans at the ocular surface. *Ocul. Surf.* **2010**, *8* (1), 8–17.

(10) Chen, L. L.; Zhou, Q.; Zhang, P. F.; Tan, W.; Li, Y. G.; Xu, Z. W.; Ma, J. F.; Kupfer, G. M.; Pei, Y. X.; Song, Q. B.; et al. Direct stimulation of de novo nucleotide synthesis by GlcNAcylation. *Nat. Chem. Biol.* **2024**, *20* (1), 19–29.

(11) Mazurov, D.; Ilinskaya, A.; Heidecker, G.; Filatov, A. Role of O-glycosylation and expression of CD43 and CD45 on the surfaces of effector T cells in human T cell leukemia virus type 1 cell-to-cell infection. *J. Virol.* **2012**, *86* (5), 2447–2458.

(12) Cervoni, G. E.; Cheng, J. J.; Stackhouse, K. A.; Heimbürg-Molinari, J.; Cummings, R. D. O-glycan recognition and function in mice and human cancers. *Biochem. J.* **2020**, *477* (8), 1541–1564.

(13) Magalhaes, A.; Duarte, H. O.; Reis, C. A. The role of O-glycosylation in human disease. *Mol. Aspects Med.* **2021**, *79*, No. 100964.

(14) Riley, N. M.; Bertozzi, C. R.; Pitteri, S. J. A pragmatic guide to enrichment strategies for mass spectrometry-based glycoproteomics. *Mol. Cell. Proteomics* **2021**, *20*, 100029.

(15) Wang, B. L.; Tsybovsky, Y.; Palczewski, K.; Chance, M. R. Reliable determination of site-specific in vivo protein N-glycosylation based on collision-induced MS/MS and chromatographic retention time. *J. Am. Soc. Mass Spectrom.* **2014**, *25* (5), 729–741.

(16) Yin, H. D.; Zhu, J. H. Methods for quantification of glycopeptides by liquid separation and mass spectrometry. *Mass Spectrom. Rev.* **2023**, *42* (2), 887–917.

(17) Wilkinson, H.; Saldova, R. Current methods for the characterization of O-glycans. *J. Proteome Res.* **2020**, *19* (10), 3890–3905.

(18) Lavery, S. B.; Steentoft, C.; Halim, A.; Narimatsu, Y.; Clausen, H.; Vakhrushev, S. Y. Advances in mass spectrometry driven O-glycoproteomics. *Biochim. Biophys. Acta* **2015**, *1850* (1), 33–42.

(19) Song, X. Z.; Ju, H.; Lasanajak, Y.; Kudelka, M. R.; Smith, D. F.; Cummings, R. D. Oxidative release of natural glycans for functional glycomics. *Nat. Methods* **2016**, *13* (6), 528–534.

(20) Vos, G. M.; Weber, J.; Sweet, I. R.; Hooijschuur, K. C.; Toraño, J. S.; Boons, G. J. Oxidative release of O-glycans under neutral conditions for analysis of glycoconjugates having base-sensitive substituents. *Anal. Chem.* **2023**, *95* (23), 8825–8833.

(21) Meng, X. J.; Pang, H. H.; Sun, F.; Jin, X. H.; Wang, B. H.; Yao, K.; Yao, L.; Wang, L. J.; Hu, Z. P. Simultaneous 3-nitrophenylhydrazine derivatization strategy of carbonyl, carboxyl and phosphoryl sub-metabolome for LC-MS/MS-based targeted metabolomics with improved sensitivity and coverage. *Anal. Chem.* **2021**, *93* (29), 10075–10083.

- (22) Xiang, L.; Ru, Y.; Shi, J. C.; Zhao, H. Z.; Huang, Y.; Cai, Z. W.; Wang, L. Derivatization of *N*-acyl glycines by 3-nitrophenylhydrazine for targeted metabolomics analysis and their application to the study of diabetes progression in mice. *Anal. Chem.* **2023**, *95* (4), 2183–2191.
- (23) Godzien, J.; Ciborowski, M.; Armitage, E. G.; Jorge, I.; Camafeita, E.; Burillo, E.; Martín-Ventura, J. L.; Rupérez, F. J.; Vázquez, J.; Barbas, C. A single in-vial dual extraction strategy for the simultaneous lipidomics and proteomics analysis of HDL and LDL fractions. *J. Proteome Res.* **2016**, *15* (6), 1762–1775.
- (24) Varki, A. Sialic acids in human health and disease. *Trends Mol. Med.* **2008**, *14* (8), 351–360.
- (25) Zhao, C. H.; Wang, X. D.; Wu, J.; Hu, Y. L.; Zhang, Q. W.; Zheng, Q. Analysis of *O*-acetylated sialic acids by 3-nitrophenylhydrazine derivatization combined with LC-MS/MS. *Anal. Methods* **2024**, *16* (16), 2472–2477.
- (26) Omori, Y.; Kon, T. Goldfish: an old and new model system to study vertebrate development, evolution and human disease. *J. Biochem.* **2019**, *165* (3), 209–218.
- (27) Yamakawa, N.; Vanbeselaere, J.; Chang, L. Y.; Yu, S. Y.; Ducrocq, L.; Harduin-Lepers, A.; Kurata, J.; Aoki-Kinoshita, K. F.; Sato, C.; Khoo, K. H.; et al. Systems glycomics of adult zebrafish identifies organ-specific sialylation and glycosylation patterns. *Nat. Commun.* **2018**, *9*, 4647.
- (28) Pongracz, T.; Verhoeven, A.; Wuhrer, M.; de Haan, N. The structure and role of lactone intermediates in linkage-specific sialic acid derivatization reactions. *Glycoconj. J.* **2021**, *8* (2), 157–166.